

## Molecular Physics

An International Journal at the Interface Between Chemistry and Physics


ISSN: 0026-8976 (Print) 1362-3028 (Online) Journal homepage: [www.tandfonline.com/journals/tmph20](http://www.tandfonline.com/journals/tmph20)


# Aqueous microdroplet chemistry enables sustainable, scalable synthesis of polyaniline

Juldeh Jallow, Xiaowei Song, Chanbasha Basheer, Umair Baig, Abdullah Alaliwi, Rashed S. Bakdash & Richard N. Zare

To cite this article: Juldeh Jallow, Xiaowei Song, Chanbasha Basheer, Umair Baig, Abdullah Alaliwi, Rashed S. Bakdash & Richard N. Zare (21 Jan 2026): Aqueous microdroplet chemistry enables sustainable, scalable synthesis of polyaniline, Molecular Physics, DOI: [10.1080/00268976.2026.2617944](https://doi.org/10.1080/00268976.2026.2617944)


To link to this article: <https://doi.org/10.1080/00268976.2026.2617944>

 View supplementary material [↗](#)

 Published online: 21 Jan 2026.

 Submit your article to this journal [↗](#)

 Article views: 87

 View related articles [↗](#)

 View Crossmark data [↗](#)

# Aqueous microdroplet chemistry enables sustainable, scalable synthesis of polyaniline

Juldeh Jallow<sup>a</sup>, Xiaowei Song<sup>b</sup>, Chanbasha Basheer<sup>a,c</sup>, Umair Baig<sup>d</sup>, Abdullah Alaliwi<sup>a</sup>, Rashed S. Bakdash<sup>c</sup> and Richard N. Zare<sup>b</sup>

<sup>a</sup>Chemistry Department, Interdisciplinary Research Center for Membranes and Water Security, King Fahd University of Petroleum and Minerals, Dhahran, Saudi Arabia; <sup>b</sup>Department of Chemistry, Stanford University, Stanford, CA, USA; <sup>c</sup>Interdisciplinary Research Center for Refining & Advanced Chemicals, King Fahd University of Petroleum and Minerals, Dhahran, Saudi Arabia; <sup>d</sup>Interdisciplinary Research Center for Membranes and Water Security, King Fahd University of Petroleum and Minerals, Dhahran, Saudi Arabia

## ABSTRACT

Polyaniline (PANI) is a widely studied conductive polymer with applications from antifouling coatings to flexible electronics. Its conventional synthesis typically relies on strong oxidants, elevated temperatures, and prolonged reaction times. Here, we introduce an innovative and sustainable method for synthesising PANI that exploits the unique chemistry of aqueous microdroplets. At the air–water interface of these microdroplets, spontaneous proton-coupled electron-transfer reactions occur in a naturally acidic, oxidative environment, converting aniline monomers into reactive anilinium cations and radicals. These transient intermediates rapidly initiate oxidative polymerisation, yielding both the emeraldine salt and base forms of PANI. To further enhance polymer yield and support scale-up, ferrous ions ( $\text{Fe}^{2+}$ ) are incorporated to catalyze the decomposition of hydrogen peroxide into hydroxyl radicals ( $\text{OH}\bullet$ ), thereby accelerating chain propagation. This ambient, interfacial approach enables complete conversion of a 50 mL, 0.4 M or 0.6 M aniline solution into gram-scale quantities of PANI within just 30 min. The resulting polymer can be directly deposited onto diverse substrates. As demonstrations of utility, PANI-coated alumina membranes achieved 95% oil rejection in oil–water separation, and PANI-modified microelectrodes exhibited ideal electrochemical behaviour. This work establishes microdroplet interfacial chemistry as a robust and generalisable strategy for green, scalable conductive polymer synthesis.

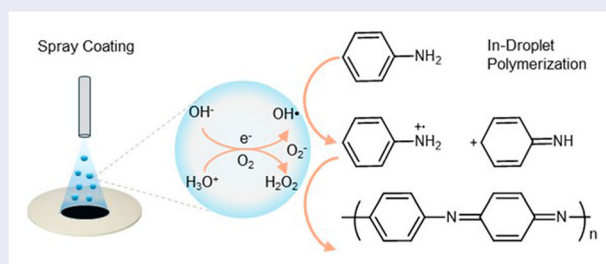
A conductive polymer (polyaniline) can be conveniently synthesised at the gram scale by taking advantage of interfacial redox potential of spraying water microdroplets under ambient conditions. This microdroplet polymerisation method shows promising potential in the on-demand coating of hydrophobic materials on any object surface.

## ARTICLE HISTORY

Received 10 October 2025  
Accepted 12 January 2026

## KEYWORDS

Conductive polymer synthesis; microdroplet chemistry; aniline; air–water interface




## Introduction

Conducting polymers are an essential family of organic compounds composed of monomer units with conjugated

chemical bonds that, upon doping, can become conductive and have become popular thanks to their unique properties [1]. They can replace metals due to their high

**CONTACT** Chanbasha Basheer  cbasheer@kfupm.edu.sa  Chemistry Department, Interdisciplinary Research Center for Refining & Advanced Chemicals, Interdisciplinary Research Center for Membranes and Water Security, King Fahd University of Petroleum and Minerals, Dhahran, 31261, Saudi Arabia; Interdisciplinary Research Center for Refining & Advanced Chemicals, King Fahd University of Petroleum and Minerals, Dhahran, 31261, Saudi Arabia; Richard N. Zare  zare@stanford.edu Department of Chemistry, Stanford University, 380 Roth Way, Stanford, CA, 94305, USA

 Supplemental data for this article can be accessed online at <https://doi.org/10.1080/00268976.2026.2617944>.

conductivity, low density, and ease of processing [2]. A critical member of this family of conducting polymers is polyaniline (PANI). PANI is unique and popularly used in research and various applications due to its simplicity, low cost [3], intrinsic electrical conductivity, high environmental stability [4], cheap and easy availability of monomers [5], high polymerisation efficiency [6], and the ability to be doped by acids [7].

For PANI synthesis, electrochemical polymerisation, and various chemical polymerisation methods have been conventionally used in bulk-phase reactions [1,2,6,7]. However, these methods are usually characterised by longer reaction times, and some are difficult to scale up, particularly for electrochemical methods. Ammonium peroxydisulfate has been widely used on a large scale to produce PANI as an oxidant [2,6]. However, the oxidant is stoichiometrically consumed in the reaction. As a result, the process demands substantial quantities of reagents for high-volume PANI production, making post-synthesis purification more challenging.

Water microdroplets can serve as highly active microreactors for organic synthesis, producing valuable materials across various fields of chemistry. They involved the production of charged droplets [8] that exhibit unique physicochemical properties at the air-liquid interface [9]. A decrease in the entropy of solute molecules, caused by their ordered orientation near the droplet surface, has been reported to influence reactivity [10,11]. Rapid solvent evaporation can further increase local solute concentration, thereby enhancing reaction rates [12,13]. Additionally, unusual dielectric properties and effective diffusion within microdroplets have been shown to accelerate reactions during material synthesis [14].

One promising application of microdroplet chemistry is to induce polymerisation [15]. Here, we report the oxidative polymerisation of polyaniline (PANI) in aqueous microdroplets using a nebulising spray-based method (Figure 1), also referred to as aerosol-assisted synthesis. Our setup includes a sprayer, an air compressor for nebulising the precursor solution, a peristaltic pump for continuous liquid recirculation, and a pressure control system to regulate droplet generation. At the air-water microdroplet interface, water undergoes radical-initiated redox reactions in the absence of catalysts or externally applied potentials [16]. This reactivity is driven by abundant reactive oxygen species (ROS) at the air-water interface, arising from the asymmetric distribution of hydronium and hydroxide ions [17,18], which are subsequently converted to hydroxyl radicals and hydrogen peroxide [19,20].

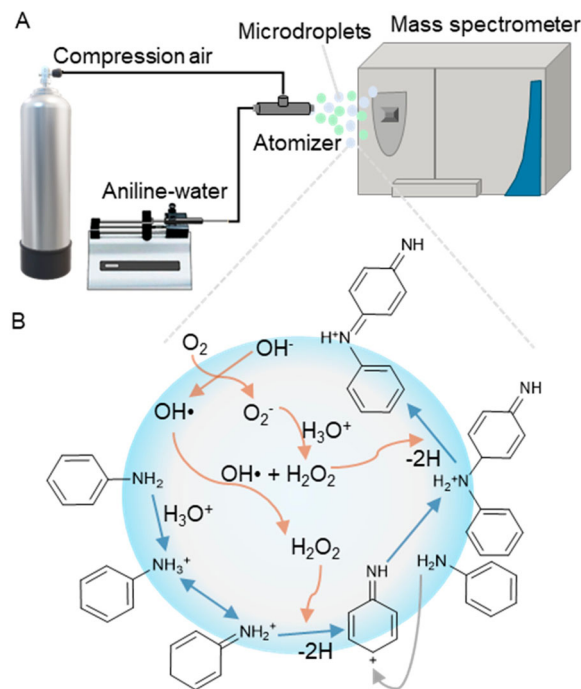


**Figure 1.** The aniline polymerisation process: (A) Schematic diagram of PANI synthesis setup; and (B) Proposed stepwise polymerisation mechanism.

## Experimental procedure

### Online MS monitoring of the PANI formation

A nebulising spray setup coupled to an Orbitrap mass spectrometer (Thermo Fisher, San Jose, US) is used to detect the stepwise oxidation and elongation of aniline. Compressed air is used as the nebulising gas to spray the aniline solution, with an average particle size of 10–30 microns. The coaxial nebulising spray system consisted of a syringe pump (Masterflex, Cole Parmer, Vernon Hills, IL, USA), a silica capillary (ID: 150  $\mu$ m, OD 250  $\mu$ m, Polymicro Technologies, Phoenix, AZ, USA), stainless steel tubing (ID: 500  $\mu$ m, OD: 2.0 mm, Length: 20 mm), and stainless-steel tee (Swagelok, Solon, OH, USA), and gas cylinder (Praxair, San Jose, CA, USA). The spray head-to-MS inlet distance was set to 15 mm. The nebulising gas pressure is set at 120 psi. The flow rate varies between 5 and 50  $\mu$ L/min.

### PANI synthesis procedure

The setup for this microdroplet synthesis of PANI includes a sprayer, a pressure-controlling system, an air compressor, and a peristaltic pump that facilitates the repeated flow of the precursor solution. 0.4 M aniline (Sigma -Aldrich Co. Ltd.) was added to 50 mL of water,

followed by 200  $\mu\text{L}$  of 1 M hydrochloride (HCl) and 0.3 M iron chloride ( $\text{FeCl}_3$ , Sigma Aldrich, Co. Ltd.). The reaction started with the reaction solution flowing from the reaction vessel through the peristaltic pump into the sprayer. Nebulisation by the air compressor produces microdroplets from the sprayer. The produced droplets return to the reaction vessel and flow through the peristaltic pump, and the cycle is repeated for 30 min. After the synthesis is complete, 20 mL of methanol and 10 mL of water are added to the resulting solution to dissolve any unreacted monomers and remove impurities. Vacuum filtration is used to obtain polyaniline. To ensure that all unreacted monomers were removed, the purification was repeated until a clear filtrate was obtained, followed by drying the PANI residue at 60  $^\circ\text{C}$  for 1 h. To optimise our reaction conditions for maximum capability, the effects of aniline monomer, HCl, and  $\text{FeCl}_3$  concentrations on the formation and conductivity of polyaniline were investigated.

### Transmission electron microscopy (TEM)

The PANI solution was filtered and washed, and TEM analysis was performed to examine the size, shape, and morphology of the synthesised material. A Scanning Electron Microscope (SEM, Thermo Scientific Quattro S, USA) was used to study the morphology and elemental composition of the PANI-coated alumina for oil–water separation. An XRD instrument (Rigaku Ultima IV, Kuraray Co., Ltd., Japan) was used to observe the decrease in crystallinity of the alumina resulting from the coating of PANI.

### $^1\text{H-NMR}$ characterisation of PANI

A 600 MHz (JEOL, Japan) spectrometer was used for the Nuclear Magnetic Resonance (NMR) study.  $^1\text{H-NMR}$  samples were prepared in  $\text{DMSO-d}_6$  as a solvent, and 200  $\mu\text{L}$  of the PANI solution was added to an NMR tube, followed by 400  $\mu\text{L}$  of  $\text{DMSO-d}_6$ . The mixture was sonicated for 30 min to ensure uniform dissolution of the PANI before analysis. To support our synthesis, we also run NMR on PANI produced by the conventional hydrothermal method. The formation of PANI is indicated by the appearance of three distinct peaks of aromatic protons at  $\delta = 7.0\text{--}7.3$  ppm. The characteristic  $\text{DMSO-d}_6$  peak is observed at  $\delta = 2.5$  ppm. The highly intense peak at  $\delta = 4.5$  ppm corresponds to water originating from the synthesis process. The N-H proton resonance peak overlapped with water molecules at around  $\delta = 4.0$  ppm, making it impossible for it to appear.

### Conductivity study

The conductivity of a PANI solution was measured. When 0.4 M aniline was used with 0.3 M  $\text{Fe}^{2+}$  and 1 M HCl, the conductivity was found to be  $5.70 \times 10^{-3}$   $\text{S cm}^{-1}$  after 30 min. The conductivity increased to  $8.79 \times 10^{-3}$   $\text{S cm}^{-1}$  when the aniline concentration was increased to 0.6 M, with the same  $\text{Fe}^{2+}$  and HCl concentrations. This clearly indicates an increase as the aniline concentration used in the polymerisation process increased. Similarly, as the reaction time was increased to 1 hr, the conductivity decreased to  $6.04 \times 10^{-3}$   $\text{S cm}^{-1}$ ; this may be due to the overoxidation of the aniline monomers in an acidic medium.

### FTIR characterisation

The surface chemistry of polyaniline samples produced from different aniline concentrations via the microdroplet synthesis route was studied using Fourier Transform Infrared Spectroscopy (FTIR). As shown in Fig. S6, the stretching vibrations of C–H  $\text{sp}^2$  and C = C modes of the benzoin groups are observed at 3054 and 1442  $\text{cm}^{-1}$ , respectively. A 1106  $\text{cm}^{-1}$  is attributed to the bending vibrations of C–H bonds, while the C–N stretching vibrations are observed at 1304  $\text{cm}^{-1}$  for aromatic conjugation. Two N–H bands are observed; the band at 3259  $\text{cm}^{-1}$  is related to its stretching modes, while the band at 1582  $\text{cm}^{-1}$  is related to the bending vibrations.

### In-situ coating of alumina ceramic membrane for oil–water separation

Due to polyaniline's rigid structure, it can form stable coatings on the alumina ceramic membrane support. The large number of amino groups and the presence of electric double layers ensure PANI's hydrophilicity and underwater superoleophobicity, which enable PANI to disperse effectively in water and allow water to filter through while rejecting oil. The membrane was prepared by in situ coating. The bare alumina ceramic membrane was washed with HCl to remove surface oxides and then rinsed with deionised water. The cleaned bare membrane was then placed in the PANI synthesis by the microdroplets process for in-situ coating during the polymerisation. After synthesis, the coated membrane was dried in an oven at 60  $^\circ\text{C}$  for 1 h. The drying temperature was maintained below the thermal stability of PANI to prevent polymer chain breakdown.

### Contact angle measurement of PANI-coated alumina membrane

To analyze the surface wettability of our membrane, which is crucial for its behaviour during fouling, we

measured the water contact angle (WCA) of pristine alumina and PANI-coated alumina ceramic membranes in air. The membranes for both M1 and M2 appeared superhydrophobic, as indicated by water contact angles (WCAs) of 0°. At the same time, the pristine alumina shows a close to 0° angle. The superhydrophilicity of the PANI/alumina ceramic support membrane is attributed to the presence of amine functional groups on its surface, which facilitate the absorption and filtration of water while rejecting oil.

### **Oil-water separation using PANI-coated alumina ceramic membrane**

Daily, large volumes of oil enter the environment from various sources, including industrial facilities, homes, and other sources. Although natural processes remove some of these oils, a significant portion contaminates water bodies, making it difficult for aquatic organisms to survive and for water to be used domestically. Oil-water mixtures exist in categories. However, emulsified oil-water mixtures tend to be more difficult to separate due to the smaller droplet diameters induced by surfactants. Separation methods, such as coagulation and flocculation, have been applied to some extent to separate oil emulsions. However, membrane filtration is more suitable due to its lower cost and better efficiency. Due to the presence of an electric double layer and the hydrophilic amine functional groups on the PANI surface, it exhibits strong adsorption and excellent oil rejection.

To demonstrate the applicability of synthesised PANI, oil-water separation was performed using a crossflow filtration system with a dead-end filtration setup (HP 4750 stirred cell, Sterlitech, US), with argon gas as the pressurising gas. The oil-water emulsion was prepared by mixing 0.2 g of diesel oil and 1.0 g of SDS in 1 L of water for 24 h. After the separation using the two membranes, we calculated the permeate flux and oil rejection using the following equations:  $\text{Flux} = \frac{V}{At}$  and  $R = \frac{C_f - C_p}{C_f} \times 100\%$  where  $V$  is the volume of permeate in litres,  $A$  is the area of the membrane in  $\text{m}^2$  and  $t$  is the time taken for measurement of permeate in hours,  $C_f$  and  $C_p$  are the oil concentrations in the feed and permeate solutions respectively. In this study, M1 and M2 refer to the alumina ceramic membranes modified with PANI prepared from 0.4 M and 0.6 M aniline, respectively.

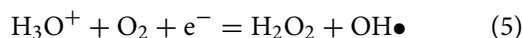
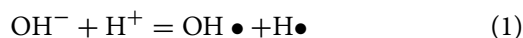
The synthesised PANI solution was sprayed onto an alumina ceramic support to form a PANI membrane for the separation of oil-water emulsions. The results of the oil-water separation confirm the effectiveness of PANI as a viable material for purifying oil-contaminated water. It

is essential to note that hydroxyl radicals are generated in two distinct instances during this reaction. We measured the oil-water separation of the membranes under various pressures and over time using total organic carbon (TOC) analysis. Table 1S. Demonstrate the performance efficiency of the PANI-coated alumina membrane with previously published literature. The 95% rejection rate is comparable to that reported for membranes in oil-water separation. PANI-coated membrane performed well due to its denser polymer network, which reduces the pore sizes of the membrane, which decreases the permeate flow and hence increases the rejection rate. The presence of amine groups from the PANI on the membrane surface also increases the hydrophilicity and hydrophobicity of the alumina membrane surface.

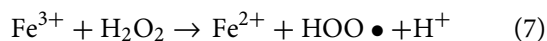
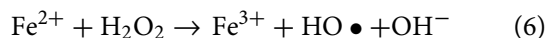
### **Results and discussion**

Microdroplets provide sufficient driving energy and an ideal interfacial environment for aniline oxidation and chain propagation. First, when high-pressure nebulising gas sprays the bulk water at a high speed, it overcomes surface tension to create numerous micron-sized droplets with a significant gain in contacting area of AWI (Figure 1A). This process uses the kinetic energy stemming from the nebulising gas to preserve huge chemical potential across the reactive microdroplets' AWI region. Meanwhile, spraying also leads to the charge separation across the droplet surface. Electrons tend to be stripped off and remain on the surface of smaller droplets, leaving larger ones with positive charge [21,22]. The strong electric field and the induced microlighting between positive and negative droplets provide an additional driving force to promote redox reactions during droplet fission and charge separation [23]. Single-electron transfer will occur between hydroxide ( $\text{OH}^-$ ) and a proton ( $\text{H}^+$ ) across the highly active AWI region to form the hydroxyl radical ( $\text{OH}\bullet$ ) and hydrogen ( $\text{H}\bullet$ ), leading to the formation of hydrogen peroxide ( $\text{H}_2\text{O}_2$ ) (equations 1, 2, and 3). This process across AWI has been observed in experimental studies [16–18] and shown to be exothermic by theoretical calculations [19,20].

It is worth noting that the presence of oxygen in the air is a good electron donor to form superoxide anion ( $\text{O}_2^-$ ) and enhance the  $\text{OH}\bullet$  and  $\text{H}_2\text{O}_2$  generation (Figure 1B) (equations 4 and 5) [24,25].



Because the generated  $\text{OH}\bullet$  is more reactive than  $\text{H}_2\text{O}_2$  and quickly consumed, the addition of  $\text{Fe}^{2+}$  reagent can effectively break the pre-formed  $\text{H}_2\text{O}_2$  back into the  $\text{OH}\bullet$  species to further provide an enhanced oxidation environment through Fenton reaction (equations 6, 7, and 8)



The principles of microdroplet interfacial chemistry are described in our previous work [18]. These include interfacial electric field enhancement, spontaneous charge separation, accelerated proton mobility, and the formation of reactive  $\text{OH}\bullet$  radicals at the air–water interface. The process of  $\text{OH}\bullet$  formation increases with the addition of  $\text{Fe}^{2+}$ .

To characterise the chain propagation progress in microdroplets, the aniline-containing water solution (400  $\mu\text{M}$ ) was directly sprayed into a high-resolution mass spectrometer (HRMS) by nebulising gas (100 psi)-assisted nozzle spray setup (Figure 1A). The aniline monomer majorly presents as the form of anilinium ( $m/z$  94.0651,  $[\text{C}_6\text{H}_5\text{NH}_2 + \text{H}]^+$ ) because of the acidification across water microdroplet interface. But its cation radical (Fig. S1,  $m/z$  93.0573,  $\text{C}_6\text{H}_5\text{NH}_2^+$ ) was also formed by being stripped off one electron in the oxidative environment of the air–water interface (AWI) region. More importantly, another critical intermediate was successfully captured at  $m/z$  92.0490 (Fig. S2), which indicated imine cation ( $[(\text{C}_6\text{H}_5\text{NH}_2-2\text{H})+\text{H}]^+$ ) formed by dehydrogenative oxidation from the anilinium in microdroplets (Figure 1B and Figure 2A) [26]. The carbon cation of this imine intermediate can attach to the amine group from another aniline monomer to form dimer ions. This process will repeatedly elongate the chain.

Various lengths of intermediate oligomers, up to the hexamer, were successfully detected in water microdroplets sprayed at the microsecond time scale. Each oligomer ion cluster contained three forms of aniline oligomers: emeraldine and its acid and base forms. (Figure 2B). Figures 2C–F display zoom-in mass spectra of the aniline dimer, trimer, tetramer, and pentamer, respectively, confirming the molecular structures of the synthesised species and the stepwise chain elongation. For each step, the starting end of the chain is activated by losing a pair of hydrogens to form the cation, followed by the nucleophilic attack by another native aniline monomer. These results indicate that microdroplets provide acidic and oxidative environments that favour ultrafast aniline polymerisation.

An off-line scale-up PANI production was conducted with an optimised solution composed of 400–600 mM aniline, 4 mM hydrochloride (HCl), and 1.2 mM ferrous chloride ( $\text{FeCl}_2$ ). The HCl was added to acidify the aniline and increase its solubility in water.  $\text{FeCl}_2$  was added to maximise  $\text{OH}\bullet$  production via classical Fenton reactions. Finally, a green precipitate began to form, indicating the formation of the emeraldine oxidation and reduction forms of PANI (Fig. S3). The continuous spray-recycle-spray process of the 50 mL reactant solution only took 30 min to finish with over 1 g PANI production (Figure 3A).

To explore the structural details and chemical shifts of the synthesised PANI, we conducted  $^1\text{H-NMR}$ . DMSO- $d_6$  was used as a solvent to dissolve the PANI. The  $^1\text{H-NMR}$  spectra of the PANI synthesised from 600 mM aniline using the microdroplet method are shown in Figure 3B. The formation of PANI is indicated by the appearance of three distinct peaks of aromatic protons at  $\delta = 7.0\text{--}7.3$  ppm. The characteristic DMSO- $d_6$  peak is observed at  $\delta = 2.5$  ppm. The highly intense peak at  $\delta = 4.5$  ppm corresponds to water originating from the synthesis process. The N-H proton resonance peak overlapped with the water molecule peak at around  $\delta = 4.0$  ppm, making it impossible to be studied separately. To compare the microdroplet methods with conventional chemical oxidative polymerisation,  $^1\text{H-NMR}$  spectra are shown in Fig. S4A and match those of PANI synthesised by  $\text{Fe}^{2+}$  using the microdroplet method (Figs. S4B and S4C).

$^1\text{H-NMR}$  characterisation of PANI prepared by (Fig S4A) conventional hydrothermal chemical polymerisation shows spectra that closely match those obtained from the droplet method at two concentrations. The NMR results confirm that PANI synthesised via the droplet method is structurally identical to that produced by the classical approach under the same temperature conditions.

A slow polymerisation occurs in the absence of  $\text{Fe}^{2+}$ , confirming that intrinsic microdroplet oxidation, driven by interfacial electric fields, proton activity, and radical formation, can initiate the oxidative coupling of aniline monomers. However, the yield of PANI is significantly lower, approximately 5–10% of the mass obtained after 3 hrs (data not shown). However, when we introduced  $\text{Fe}^{2+}$ , the reaction yield of MOF increased with the microdroplet-induced oxidation (rapid initiation) and  $\text{Fe}^{2+}\text{--H}_2\text{O}_2$  Fenton cycling (accelerated propagation and radical regeneration).

X-ray diffraction (XRD) spectra of the pristine membrane and membranes treated with 0.4 M (M1) and 0.6 M (M2) aniline solutions indicate that the PANI deposition affects the membrane's crystallinity (Figure 3C). Fourier

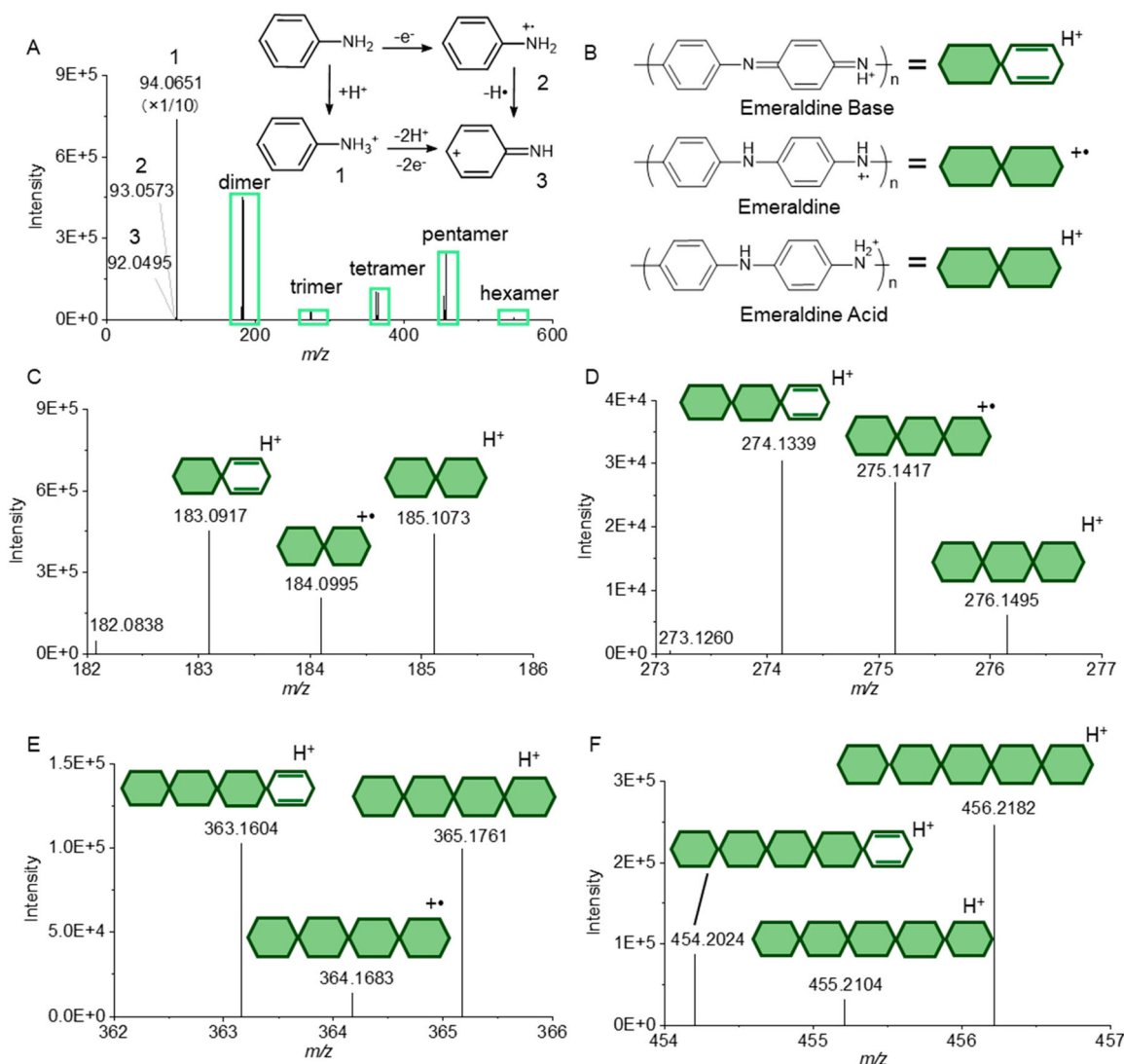


**Figure 2.** Characterisation of the aniline polymerisation process by high-resolution mass spectrometry: (A) full scan spectrum capturing the aniline monomer to hexamer; (B) the structures of three types of aniline oligomers and their symbols; (C-F) zoomed-in mass spectrum of emeraldine oxidation and reduction forms of the dimer to hexamer.

transform infrared spectroscopy (FTIR) (Figure 3D) confirms the presence of characteristic PANI functional groups on the modified membranes. The stretching vibrations of C–H  $sp^2$  and C = C modes of the benzoin groups are observed at 3054 and 1442  $cm^{-1}$ , respectively. A 1106  $cm^{-1}$  is attributed to the bending vibrations of C–H bonds, while the C–N stretching vibrations are observed at 1304  $cm^{-1}$  for aromatic conjugation. Two N–H bands are observed; the band at 3259  $cm^{-1}$  is related to its stretching modes, while the band at 1582  $cm^{-1}$  is related to the bending vibrations.

A transmission electron microscope (TEM) was used to study the morphology and structure of the synthesised PANI (Figure 3E). The morphology of PANI changes as the concentration of aniline used in the reaction increases. M1 (0.4 M) shows a crowded crystalline

fibrous structure at low magnification (200 nm). When the concentration is increased from 0.4 M to 0.6 M (M2), PANI nanofibers agglomerate and twist into wrinkled, interconnected networks [27–29]. Dark spots observed on the structures indicate the multilayer PANI, while low-density areas are associated with the exfoliation of PANI nanostructures [30]. PANI, which is known for its electrical conductivity, was the subject of our rigorous experiment. We measured the electrical conductivity of microdroplet-assisted-synthesised PANI by dipping a Whatman filter paper in PANI and drying it at room temperature. This paper, now conductive, was used as a working electrode.

As a further test of the PANI made by our method, we coated the working electrode with PANI ink and tested its conductivity by cyclic voltammetry (CV). An ideal

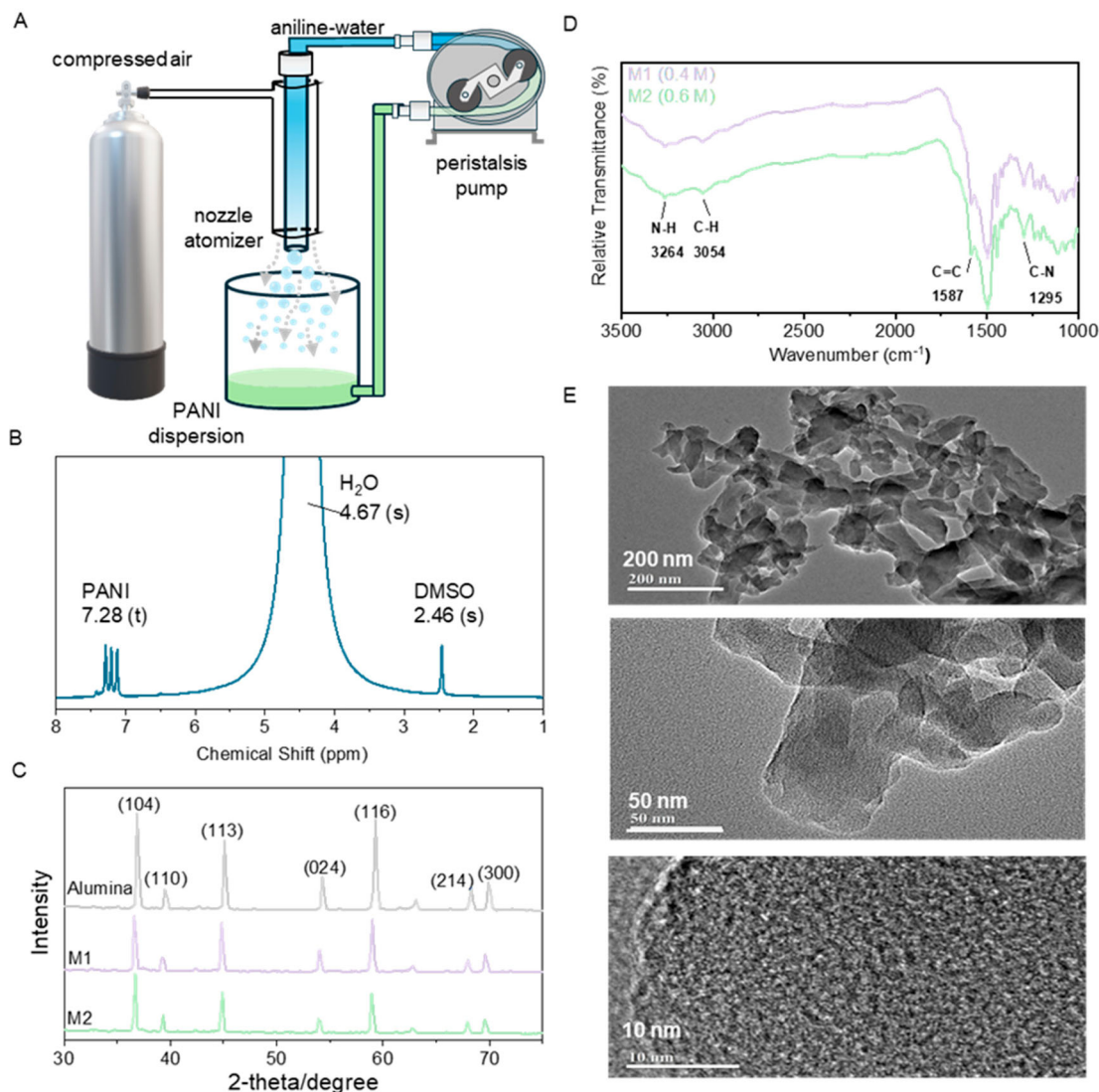


**Figure 3.** The scaled-up production of PANI and material characterisation. (A) Diagram of the PANI synthesis process. The recyclable setup consists of a microdroplet sprayer, a peristaltic pump, and an air compressor (B)  $^1\text{H-NMR}$  results of PANI produced from 0.6 M aniline using ferrous ions ( $\text{Fe}^{2+}$ ) are incorporated reaction in water microdroplets at room temperature (C) XRD of alumina ceramic support, (M1) PANI produced from 0.4 M aniline, (M2) PANI produced from 0.6 M aniline, coated on the ceramic support. (D) FT-IR of the polyaniline produced from different aniline concentrations in PANI synthesis at room temperature. (E) TEM results of PANI produced from 0.6 M aniline by water microdroplets at room temperature. Lower magnification shows the crystalline fibrous structure of PANI.

CV curve can be plotted as shown in Figure 4A, which compares a commercial corrosion inhibitor (amino tri(methylenephosphonic acid)) with the nonconductive nature of paper. Additionally, the conductivity of the PANI solution was measured and reported in the supplementary material. This key finding further validates our experimental approach.

Another test is to screen print a plastic board with PANI. As expected, a parallel circuit made of PANI conducting wires lights three LEDs, as shown in Figure 4B.

Because our PANI synthesis method enables in situ coating of material surfaces, we applied it to a microporous alumina ceramic membrane (20  $\mu\text{m}$ ), which is

mechanically robust and chemically stable. However, such membranes often possess inherently hydrophobic surfaces and large pore sizes, limiting their effectiveness in oil–water separation, particularly for emulsified oils. In-situ polymerisation of PANI during water microdroplet synthesis overcomes these limitations by introducing a hydrophilic and selective surface layer that enhances water permeability while repelling oil [31]. Additionally, the PANI coating enables pore-size modulation, improving separation efficiency and reducing oil fouling. Figure 5A shows the alumina membrane before and after in-situ PANI polymerisation, revealing a uniform surface coating. The alumina membrane was

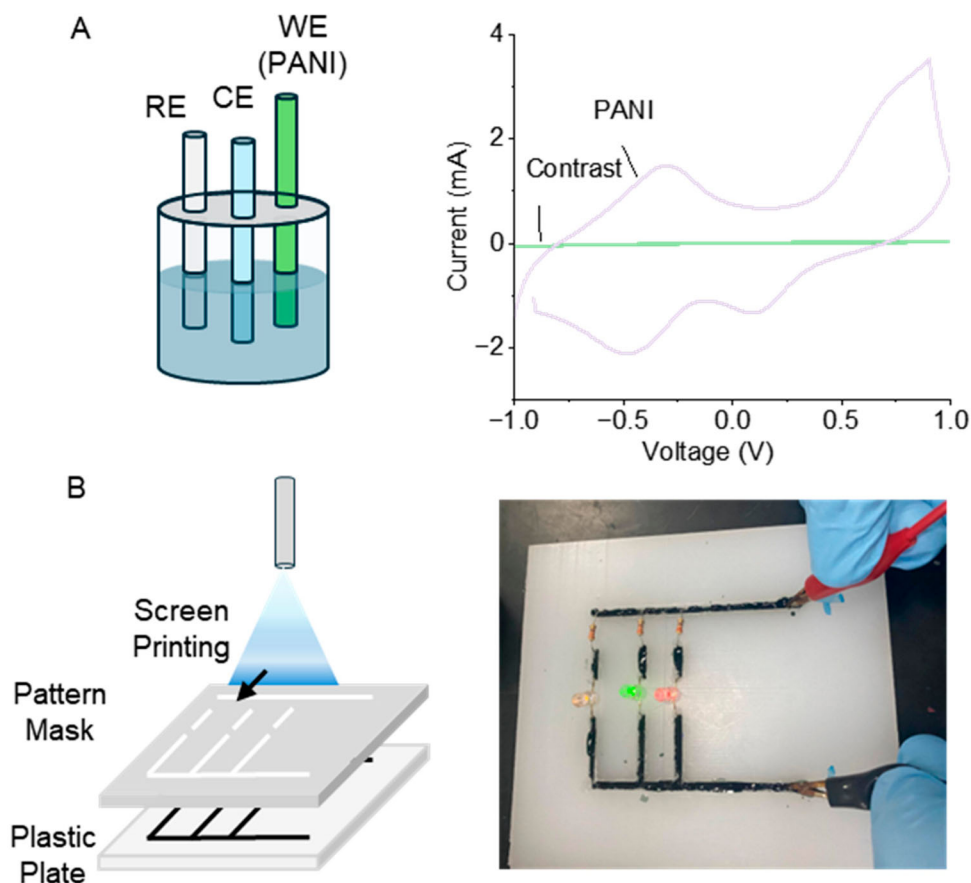


**Figure 4.** Testing the conductivity performance of the synthesised PANI materials. (A) The use of PANI as the working electrode for the cyclic voltammetry (CV) test. The AgCl/Ag and graphite were used as the counter electrode (CE) and reference electrode (RE), respectively. (B) The use of PANI for screen printing the electric board on a plastic plate, which showed perfect conductivity by turning on three LED lights in the parallel circuit.

suspended inside the spray bottle to enable in situ coating of PANI on its surface. To achieve a uniform coating, the membrane disc was positioned to ensure complete coverage across its entire area. The resulting PANI-coated alumina membrane exhibited an entirely uniform coating, making it an ideal candidate for oil/water separation applications.

After successfully characterising the modified alumina ceramic membrane loaded with PANI, separation was performed using a crossflow filtration system with a dead-end filtration setup. The membranes were first tested by measuring the effect of transmembrane pressure on the DI water flux through M1 and M2 (without oil). As expected, the pure water flux increased with increasing transmembrane pressure (Figure 5B). The highest flux was observed for M1, with a flux measured value of  $2303 \text{ L m}^{-2} \text{ h}^{-1}$  and  $1197 \text{ L m}^{-2} \text{ h}^{-1}$  for M2 at 2 bar pressure. M2 reduces water flux by blocking pores, increasing membrane thickness, and flow resistance, compared to M1.

To mimic the real oil/water mixture, an emulsion was prepared by mixing 0.5 g of sodium dodecyl sulfate

with 1 g of diesel oil in 1 L of water. The emulsified oil droplets (typically  $< 20 \mu\text{m}$ ) are stable and difficult to separate, making this scenario more challenging and less practical than simple bulk-phase separation. Emulsified samples were studied at different pressures with M1 and M2 filters. The permeation flux increases with increased transmembrane pressure, there is a considerable decrease in flux observed from the emulsion compared to that of the flux of pure water (Figure 5C). This may be caused by the fouling of the membrane resulting from the presence of oil droplets navigating into its pores, as the oil is emulsified into tiny droplets that may eventually fit into particular pores of the membrane [9]. A higher permeation flux was observed in M1 than in M2, with the highest flux values recorded as  $450 \text{ L m}^{-2} \text{ h}^{-1}$  and  $345 \text{ L m}^{-2} \text{ h}^{-1}$ , respectively, for the oil-water emulsion. We also recorded the permeation flux of the emulsion at 1 bar over 1 min at various time intervals, with measurements taken up to 135 min (Figure 5D). This behaviour is also attributed to the continuous fouling of the membrane over time, which reduces its ability to allow water to pass through its pores. The general

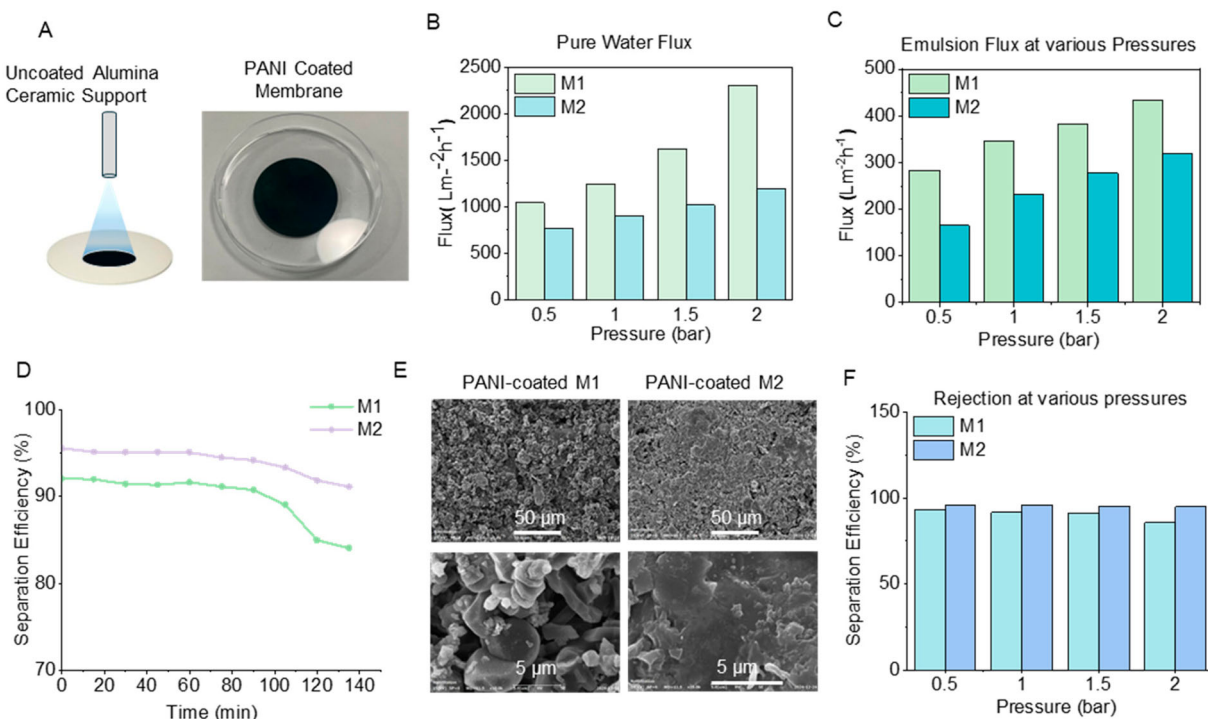


**Figure 5.** Surface PANI coating and oil-suppression performance evaluation. (A) the pristine ceramic alumina support and the PANI-coated alumina membrane (M2); (B) the permeate flux of pure water through the membranes; (C) the permeate flux of oil/water emulsions at various applied pressures; (D) the operational stability of the PANI-coated membranes during repeated oil/water separation cycles at 1 bar, measured over a 1-minute permeate volume interval; (E) SEM micrographs of the PANI-coated membrane before and after oil/water separation, alongside the M2 membrane before and after 60 min of continuous separation and (F) the separation efficiency of oil/water emulsions as a function of pressure.

increase in permeation flux with increased pressure is expected. Scanning electron micrographs (SEM) illustrate the morphology of PANI-coated membranes prepared with M1 and M2 concentrations before and after separation (Figure 5E). The presence of number of amine (-NH-) and imine (=N-) functional groups (Fig. S5), elemental mapping of the membranes (Fig. S6), and contact angle measurements (Fig. S7) further support the enhanced functionality and stability of the M2 membrane. This improved performance is expected, as mass transfer in the filtration system is directly proportional to the applied pressure. In the summary of characterisation, FT-IR confirms benzenoid and quinoid ring structures characteristic of emeraldine PANI; MS identifies early oligomers critical to mechanistic understanding; NMR demonstrates the disappearance of monomeric aromatic signatures; TEM reveals nanofiber-like morphology; and XRD shows semi-crystalline features typical of PANI.

The M2 membrane exhibited superior performance in the cross-flow oil-water separation system. Finally, we measured oil-water separation of the membranes at various pressures and over different time points using total organic carbon analysis. The separation efficiency of M2 remains constant at 95% across all pressures, whereas the

highest value for M1 was observed around 92%, decreasing to approximately 86% at 2 bars (Figure 5F). The M2 membrane surface has higher functional groups and oleophobicity, which help increase rejection. The separation efficiency of M2 was compared with previously reported studies and reported in Supplementary Table 1. Compared to other PANI coating methods, such as classical dip-coating, in situ polymer coating provides stronger adhesion, greater uniformity, and longer operational stability, making ceramic membranes more effective and durable for treating oily water samples.

## Conclusion

We have demonstrated a novel and environmentally friendly strategy for synthesising polyaniline (PANI) via oxidative polymerisation in highly reactive water microdroplets at room temperature. This microdroplet-based approach eliminates the need for high-temperature conditions and represents a significant departure from conventional synthesis routes. The effect of hydrogen peroxide generation in sprayed microdroplets can be further enhanced by coupling with the Fe<sup>2+</sup>-triggered Fenton reaction to produce hydroxyl radicals that maximise the

oxidative polymerisation of aniline. The resulting PANI exhibits good electrical conductivity and, when coated in situ onto alumina ceramic membranes, imparts excellent oil–water separation performance. The modified membranes maintained high stability across a range of applied pressures and achieved up to 95% oil rejection efficiency. Increasing the aniline concentration during synthesis led to a denser polymer layer, which, in turn, enhanced rejection efficiency but slightly reduced flux. This result is attributed to reduced pore size from thicker PANI coatings. This work highlights the potential of microdroplet interfacial chemistry as a scalable and tunable platform for the synthesis and direct functionalization of advanced separation membranes.

### Author contributions

X.S. and J.J. contributed equally to this work. C.B. designed the research; J.J., X.S., R.S., and U.B. performed the PANI preparation, FTIR, XRD, MS, SEM, TEM, and CV characterisation; J.J. drafted the initial version of the manuscript; X.S. drew all the figures; X.S., C.B., and R.N.Z. revised the paper.

### Acknowledgements

C.B. thanks the Deanship of Research at KFUPM for the Sustainable Future Consortium grant SUFC2303 and KFUPM International Summer Research Program (ISP241-CHEM-829). R.N.Z. acknowledged the Air Force Office of Scientific Research through the Multidisciplinary University Research Initiative program (AFOSR FA9550-21-1-0170) and the Sustainability Accelerator Program supported by the Stanford Doerr School of Sustainability.

### Disclosure statement

No potential conflict of interest was reported by the author(s).

### Funding

This work was supported by Sustainability Accelerator Program: [Grant Number GHG-0030-R.N.Z.]; KFUPM International Summer Research Program: [Grant Number ISP241-CHEM-829]; Sustainable Future Consortium grant: [Grant Number SUFC2303]; Multidisciplinary University Research Initiative program: [Grant Number AFOSR FA9550-21-1-0170].

### Data availability statement

The authors confirm that the data supporting the findings of this study are available within the main text and supporting information.

### References

- [1] M.L. Mota, A. Carrillo, A.J. Verdugo, A. Olivas, J.M. Guerrero, E.C. De la Cruz and N. Noriega Ramírez, *Molecules*. **24**, 1621 (2019). doi:10.3390/molecules24081621
- [2] Z.A. Boeva and V.G. Sergeev, *Polym. Sci. Ser. C*. **56**, 144–153 (2014). doi:10.1134/S1811238214010032
- [3] D.A. Zatale, S.T. Rathod and K.N. Pawar, *Int. J. Sci. Res. Sci. Technol.* **8**, 113–1116 (2021). doi:10.32628/IJSRST218328
- [4] C. Park, C. Lee and O. Kwon, *Polymers*. **8**, 249 (2016). doi:10.3390/polym8070249
- [5] I.J. Gómez, M. Vázquez Sulleiro, D. Mantione and N. Alegret, *Polymers*. **13**, 745 (2021). doi:10.3390/polym13050745
- [6] I. Karbownik, O. Rac-Rumijowska, M. Fiedot-Toboła, T. Rybicki and H. Teterycz, *Materials*. **12**, 664 (2019). doi:10.3390/ma12040664
- [7] D.W. Hatchett, M. Josowicz and J. Janata, *J. Phys. Chem. B*. **103**, 10992–10998 (1999). doi:10.1021/jp991110z
- [8] X. Yan, R.M. Bain and R.G. Cooks, *Angew. Chem. Int. Ed.* **55**, 12960–12972 (2016). doi:10.1002/anie.201602270
- [9] Z. Wei, Y. Li, R.G. Cooks and X. Yan, *Annu. Rev. Phys. Chem.* **71**, 31–51 (2020). doi:10.1146/annurev-physchem-121319-110654
- [10] S. Mondal, S. Acharya, R. Biswas, B. Bagchi and R.N. Zare, *J. Chem. Phys.* **148**, 244704 (2018). doi:10.1063/1.5030114
- [11] X. Yan, *Int. J. Mass Spectrom.* **468**, 116639 (2021). doi:10.1016/j.ijms.2021.116639
- [12] S. Banerjee and R.N. Zare, *Angew. Chem. Int. Ed.* **54**, 15008–15012 (2015). doi:10.1002/ange.201507805
- [13] X. Yan, R. Augusti, X. Li and R.G. Cooks, *ChemPlus Chem.* **78**, 1142–1148 (2013). doi:10.1002/cplu.201300172
- [14] R.A. LaCour, J.P. Heindel, R. Zhao and T. Head-Gordon, *J. Am. Chem. Soc.* **147**, 6299–6317 (2025). doi:10.1021/jacs.4c15493
- [15] K. Lee, H.R. Lee, Y.H. Kim, J. Park, S. Cho, S. Li, M. Seo and S.Q. Choi, *ACS Cent. Sci.* **8**, 1265–1271 (2022). doi:10.1021/acscentsci.2c00694
- [16] S. Jin, H. Chen, X. Yuan, D. Xing, R. Wang, L. Zhao, D. Zhang, C. Gong, C. Zhu, X. Gao, Y. Chen and X. Zhang, *JACS Au*. **3**, 1563–1571 (2023). doi:10.1021/jacsau.3c00191
- [17] M.A. Mehrgardi, M. Mofidfar and R.N. Zare, *J. Am. Chem. Soc.* **144**, 7606–7609 (2022). doi:10.1021/jacs.2c02890
- [18] H. Xiong, J.K. Lee, R.N. Zare and W. Min, *J. Phys. Chem. Lett.* **11**, 7423–7428 (2020). doi:10.1021/acs.jpcllett.0c02061
- [19] A.J. Colussi, *J. Am. Chem. Soc.* **145**, 16315–16317 (2023). doi:10.1021/jacs.3c04643
- [20] J.K. Lee, K.L. Walker, H.S. Han, J. Kang, F.B. Prinz, R.M. Waymouth, H.G. Nam and R.N. Zare, *Proc. Natl. Acad. Sci.* **116**, 19294–19298 (2019). doi:10.1073/pnas.1911883116
- [21] L.W. Zilch, J.T. Maze, J.W. Smith, G.E. Ewing and M.F. Jarrold, *J. Phys. Chem. A*. **112**, 13352–13363 (2008). doi:10.1021/jp806995h
- [22] Y. Xia, J. Xu, J. Li, B. Chen, Y. Dai and R.N. Zare, *J. Phys. Chem. A*. **128**, 5684–5690 (2024). doi:10.1021/acs.jpca.4c02981

- [23] Y. Meng, Y. Xia, J. Xu and R.N. Zare, *Sci. Adv.* **11**, eadt8979 (2025). doi:10.1126/sciadv.adt8979
- [24] A. Asserghine, A. Baby, J. N'Diaye, A.I. Romo, S. Das, C.A. Litts, P.K. Jain and J. Rodríguez-López, *J. Am. Chem. Soc.* **147**, 11851–11858 (2025). doi:10.1021/jacs.4c16759
- [25] X. Song, C. Basheer, J. Xu, M.M. Adam and R.N. Zare, *Adv. Sci.* **12**, 2412246 (2025). doi:10.1002/advs.202412246
- [26] P. Skurski and J. Simons, *J. Chem. Phys.* **160**, 034708 (2024). doi:10.1063/5.0188908
- [27] M. Liu, J. Li and Z. Guo, *J. Colloid Interface Sci.* **467**, 261–270 (2016). doi:10.1016/j.jcis.2016.01.024
- [28] S.S. Bangade, V.M. Raut, S.E. Bhandarkar and D.P. Gulwade, *Materials Today: Proc.* **29**, 1067–1070 (2020).
- [29] A. Abdelraheem, A.H. El-Shazly and M.F. Elkady, *Alex. Eng. J.* **57**, 3291–3297 (2018). doi:10.1016/j.aej.2018.01.012
- [30] M. Fuseini, M.M.Y. Zaghoul, M.F. Elkady and A.H. El-Shazly, *J. Mater. Sci.* **57**, 6085–6101 (2022). doi:10.1007/s10853-022-06994-3
- [31] J. Cui, Z. Zhou, A. Xie, M. Meng, Y. Cui, S. Liu, J. Lu, S. Zhou, Y. Yan and H. Dong, *Sep. Purif. Technol.* **209**, 434–442 (2019). doi:10.1016/j.seppur.2018.03.054